



Structure of Titan's low altitude ionized layer from the Relaxation Probe onboard HUYGENS

J.J. López-Moreno, G.J. Molina-Cuberos, Michel Hamelin, R. Grard,
Fernando Simões, R. Godard, K. Schwingenschuh, Christian Béghin,
Jean-Jacques Berthelier, V.J.G. Brown, et al.

► To cite this version:

J.J. López-Moreno, G.J. Molina-Cuberos, Michel Hamelin, R. Grard, Fernando Simões, et al.. Structure of Titan's low altitude ionized layer from the Relaxation Probe onboard HUYGENS. *Geophysical Research Letters*, 2008, 35 (22), pp.L22104. 10.1029/2008GL035338 . hal-00340606

HAL Id: hal-00340606

<https://hal.science/hal-00340606>

Submitted on 6 Feb 2016

HAL is a multi-disciplinary open access archive for the deposit and dissemination of scientific research documents, whether they are published or not. The documents may come from teaching and research institutions in France or abroad, or from public or private research centers.

L'archive ouverte pluridisciplinaire **HAL**, est destinée au dépôt et à la diffusion de documents scientifiques de niveau recherche, publiés ou non, émanant des établissements d'enseignement et de recherche français ou étrangers, des laboratoires publics ou privés.

Structure of Titan's low altitude ionized layer from the Relaxation Probe onboard Huygens

J. J. López-Moreno,¹ G. J. Molina-Cuberos,^{1,2} M. Hamelin,³ R. Grard,⁴ F. Simões,³ R. Godard,⁵ K. Schwingenschuh,⁶ C. Béghin,⁷ J. J. Berthelier,³ V. J. G. Brown,¹ P. Falkner,⁴ F. Ferri,⁸ M. Fulchignoni,⁹ I. Jernej,⁶ J. M. Jerónimo,¹ R. Rodrigo,¹ and R. Trautner⁴

Received 14 July 2008; revised 30 September 2008; accepted 13 October 2008; published 21 November 2008.

[1] Some of the secrets of the atmosphere of Titan have been unveiled by the Huygens Probe. The Permittivity Wave and Altimetry system detected a hidden ionosphere much below the main ionosphere, that lies between 600 and 2000 km. Theoretical models predicted a low altitude ionosphere produced by cosmic rays that, contrary to magnetospheric particles and UV photons, are able to penetrate down in the atmosphere. Two sensors: Mutual Impedance (MI) and Relaxation Probe (RP) measured the conductivity of the ionosphere by two different methods and were able to discriminate the two branches of electrical conductivity due to the positive and negative charges. The measurements were made from 140 to 40 km and show a maximum of charge densities $\approx 2 \times 10^9 \text{ m}^{-3}$ positive ions and $\approx 450 \times 10^6 \text{ m}^{-3}$ electrons at around 65 km. Here we present the altitude distribution of the concentration of positive ions and electrons obtained from the RP and MI sensors. **Citation:** López-Moreno, J. J., et al. (2008), Structure of Titan's low altitude ionized layer from the Relaxation Probe onboard Huygens, *Geophys. Res. Lett.*, 35, L22104, doi:10.1029/2008GL035338.

1. Introduction

[2] Titan, the largest satellite of Saturn (and the second largest in the Solar System) was discovered by Huygens in 1655. Titan, similarly to the Earth, has a dense atmosphere that is mainly composed of molecular nitrogen. On 14 January 2005, the ESA Probe Huygens entered Titan's atmosphere with the objective of determining the physical properties of its atmosphere and surface. Huygens houses the Permittivity Wave and Altimetry (PWA), a subsystem of the Huygens Atmospheric Structure Instrument (HASI) devoted to the investigation of the electric properties and electromagnetic phenomena in the atmosphere below 170 km and on the surface [Fulchignoni et al., 2005].

[3] The structure of the ionosphere of Titan has intrigued planetologists for a long time. The possibility of electrical discharges in the atmosphere has also been of great interest from before the Voyager encounters with Titan [Gupta et al., 1981]. The ionosphere was detected by the radio occultation experiment during the Voyager 1 encounter in 1980 [Bird et al., 1997] and it has been sounded several times since the first Cassini Orbiter encounter on October, 2004 [Mahaffy, 2005], where the ionospheric electron densities and temperatures were measured [Wahlund et al., 2005]. The ionospheric composition has been measured by the Ion and Neutral Mass Spectrometer (INMS) instrument [Cravens et al., 2006], the total ion density agrees quite well with the electron density obtained by the Radio and Plasma Wave Science (RPWS) instrument. Coates et al. [2007] revealed the existence of negative ions with densities up to $\sim 100 \text{ cm}^{-3}$. The Radio Science (RSS) Experiment on board Cassini shows the presence of intermittent ionospheric layers with electron densities up to 2000 cm^{-3} between 500 and 900 km [Kliore, 2007]. The RPWS instrument on board Cassini has not detected any radio signal of lightning after 35 close Titan flybys [Fischer et al., 2007].

[4] Three sources contribute to the ionization of Titan's atmosphere: ultraviolet radiation from the Sun, charge precipitation from Saturn's magnetosphere, and galactic cosmic rays. The first two mechanisms are not efficient at altitudes below 400 km and their role is therefore not appreciable in the range covered by PWA. Electricity in the chemistry of the Titan atmosphere is of main importance. Ions involved in the reactions controlling the composition and evolution of the atmosphere can give rise to the formation of complex polymers [Vuitton et al., 2006].

[5] Theoretical models [Borucki et al., 1987; Molina-Cuberos et al., 1999a, 1999b] predict that cosmic rays can penetrate the lower atmosphere and induce an ionosphere below 400 km. Borucki et al. [1987] calculated a peak electron density of 1600 cm^{-3} at 95 km and showed that aerosols could appreciably reduce the density. Molina-Cuberos et al. [1999a, 1999b, 2000] modeled the ion-neutral chemistry of the lower ionosphere and calculated the concentrations of electrons and positive and negative ions depending on factors such as the electron recombination rate, the modulation of cosmic rays by the solar wind, the nature of the major cations and the concentration of electrophilic species. The ionospheric models have recently been updated. Using improved aerosol density profiles Borucki and Whitten [2008] found the peak of electron density at 80 km.

¹Instituto de Astrofísica de Andalucía, CSIC, Granada, Spain.

²Electromagnetismo, Facultad de Químicas, Universidad de Murcia, Murcia, Spain.

³CETP, IPSL, Saint Maur, France.

⁴RSSD, ESTEC, European Space Agency, Noordwijk, Netherlands.

⁵Department of Mathematics and Computer Science, Royal Military College of Canada, Kingston, Ontario, Canada.

⁶Space Research Institute, OEAW, Graz, Austria.

⁷LPCE, CNRS, Orléans, France.

⁸CISAS "G. Colombo", Università di Padova, Padua, Italy.

⁹LESIA, Observatoire de Paris, Meudon, France.

[6] The upper ionosphere of Titan was explored by Voyager and, more recently, by Cassini. However no information was available about the lower ionosphere before the descent of Huygens. In this paper we report the concentration of electrons and positively charged particles derived from the conductivity measurements obtained by the Mutual Impedance (MI) and Relaxation Probe (RP) sensors of HASI below 140 km.

2. Electrical Conductivity and Charge Concentrations

[7] The PWA subsystem consists of a four-electrode MI probe and a double RP including two sensors RP1 and RP2 that measured the permittivity and conductivity of the environment, detected electromagnetic waves, and static electric fields [Grard *et al.*, 2006]. The instrument was tested in the atmosphere of the Earth during several balloon campaigns using a mock-up of the Huygens Probe. The results obtained during these campaigns confirmed the validity of the experiment and the functionality of the instrument [López-Moreno *et al.*, 2001, 2002].

[8] The relaxation technique for measuring the small ion polar conductivities, known also as the “transient response method”, depends only on the determination of a time constant and not on calibration [Ogawa, 1985]. The experimental set-up consists of an electrode exposed to the ionized medium that is momentarily biased at a negative or positive potential with respect to a reference level, that of the Huygens Probe structure. The sensor subsequently returns to its initial equilibrium by collecting positive or negative ambient charges. The sequence of measurements consists of four relaxation cycles of 56 s, where the source potential is successively set to +5, 0, −5 and 0 V. When space charge effects are neglected and the reference level is stable, the potential difference between the RP electrode and the Huygens Probe follows an exponential law of the type:

$$V = (V_0 - V_f) \exp(-t/\tau) + V_f, \quad (1)$$

where V_0 and V_f are the initial and floating potentials, respectively. The time constant, τ , is related to the resistance, R_e , and capacitance, C_e , of the electrode in the plasma by $\tau = R_e C_e$.

[9] The slope of the potential decay, or time constant τ , provides the polar components of the electrical conductivity $\sigma = \epsilon_0/\tau$, where ϵ_0 is the permittivity of vacuum [Grard *et al.*, 2006; López-Moreno *et al.*, 2001]. A discrete capacitor $C_p = 352$ pF is connected in parallel with the RP2 sensor, in order to reduce the speed of decay for a given conductivity, thus extending the range of measurements towards larger conductivities by a factor of $(C_e + C_p)/C_e$.

[10] When the ratio of the electrode dimension over the Debye length is large, the neutral medium approximation is no longer valid. It is necessary to take into account the fact that the resistance and capacitance of the electrode are not constant and depend upon electrode potential, charge density and Debye length. In this situation, the potential around the sensor does not obey a Laplace field, but a Poisson field is obtained by solving the continuity, flux and Poisson equations for repelled and attracted charges.

The potential difference between the RP electrode and the Huygens Probe satisfies the differential equation [Godard, 2007]:

$$I = \frac{V}{R} = -\frac{dQ}{dt} = -\frac{d}{dt}(CV) = -\frac{dC}{dt}V - C\frac{dV}{dt}, \quad (2)$$

where I is the collected current, Q is the charge of the electrode and C is capacitance of the electrode. Equation (2) is solved with an implicit scheme: first the signal is simulated numerically; then the electric conductivity and the number density of the charged species are deduced using optimization techniques. The minimization function is unimodal and forms a cusp near the global minimum, which makes all standard minimization routines ill conditioned. From this very careful analysis, we have obtained almost perfect fits between experimental and simulated signals. However, very minor discrepancies at large potentials, and for short periods of time, were sometimes observed. They absolutely did not affect data processing. We do not know exactly the cause of these minor discrepancies. They may be explained in terms of interactions between the electrode, the boom, and the gondola, or could reflect the fact that the reference potential was not stable at large potentials.

[11] The Huygens Probe sent the measurements collected with the two relaxation probes to the Cassini Orbiter through Channel A (RP1) and Channel B (RP2). Unfortunately Channel A was not recorded and only the measurements performed with RP2, the electrode designed for large conductivities, are available. The first RP data package was stored into the onboard Huygens memory at an altitude of ≈ 139 km, and the instrument collected and transmitted subsequent data set during the whole descent, until impact. We present the analyses of 11 data set with $V_0 = 5$ V and 5 data set with $V_0 = -5$ V, covering the altitude ranges 130–40 km and 130–65 km, respectively. Outside these ranges, the ambient electric conductivity was lower than 5×10^{-13} Sm^{−1}, too low to be measured with RP2.

[12] Several relaxation curves show an anomalous behaviour with the occurrence of “plateaus” in the $V(t)$ characteristics, i.e., intervals of times during which the potential of the probe with respect to Huygens displays no variations in time. The probe potential thus remains within the range of one digital step (0.1 V) during 6 to 32 s, at altitudes of 99.7 ± 1.3 km, 71.9 ± 0.3 km and 57.76 ± 0.07 km, for example [see Grard *et al.*, 2006, Figure 3]. The nature of such plateaus is uncertain. They could reflect the presence of small clouds, with typical dimensions of 140 to 600 m, where the aerosol concentration is such that the electrical conductivity lies below the instrument sensitivity threshold ($\sim 5 \times 10^{-13}$ Sm^{−1}). The longest plateau is seen at altitudes between 101 and 97 km when the voltage changes by merely 0.2 V in 56 s. The plateaus are ignored in the calculation of the electrical conductivity, because they are anomalies in an otherwise continuous and homogeneous ionosphere. The probe descent speed varies from changes from 70 m/s at 100 km to 30 m/s at 65 km.

[13] Figure 1 shows the polar components of the electrical conductivity as functions of altitude. We observe that $\sigma^- \gg \sigma^+$, which is due to the presence of electrons, that

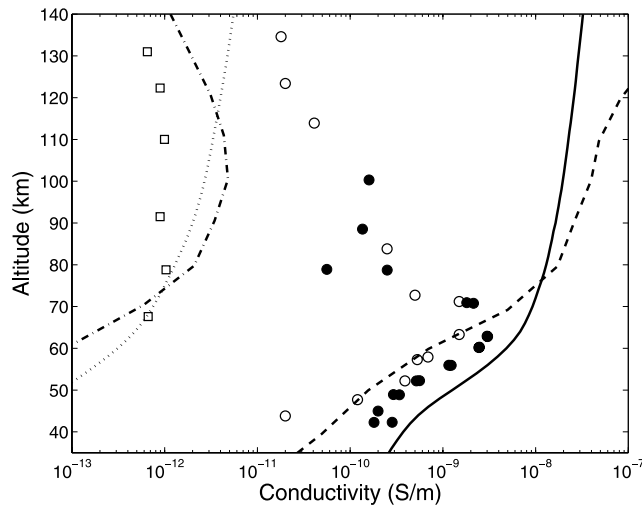


Figure 1. The two components of the conductivity of the atmosphere of Titan between 40 and 140 km altitude: positive charges (empty squares) and negative charges (empty circles) measured by RP2, and negative charges measured by MI (solid circles). Lines show the conductivity predicted by *Molina-Cuberos et al.* [1999a], dotted (σ^+) and solid, (σ^-) and by *Borucki and Whitten* [2008], dash-dotted (σ^+) and dashed (σ^-).

were predicted as the most abundant negative charges in the atmosphere, and corroborate the results independently obtained with the MI probe [Hamelin et al., 2007]. Figure 1 also shows the results that two models give for the two branches of the conductivity. The model by *Molina-Cuberos et al.* [1999a], does not consider the presence of aerosols and shows an ionospheric layer mainly formed by covalently bound ions. The model by *Borucki and Whitten* [2008] includes the presence of aerosols and photoelectron emission. For the plot we have selected the profile obtained by using the parameters which better fits the measurements obtained by HASI, i.e., a constant mass flux of aerosols of $2.0 \times 10^{-12} \text{ kg m}^{-2} \text{ s}^{-1}$, a particle density of 420 kg m^{-3} and a photoemission threshold of 7.2 eV, see reference for details. Aerosols affect the conductivity by decreasing the electron and ion concentration due to capture process. Simultaneously the concentration is increased by UV photoelectron emission. We observe that below 65 km the conductivity due to electrons is inside of a band limited by the theoretical models, however above ≈ 70 km the observed conductivity is much lower than the predictions. The positive branch of conductivity was measured above 65 km and we can observe that the measured conductivity is smaller than those obtained by both models.

[14] The electrical conductivities due to positive and negative charges are related to the concentration and mobility of the ions and electrons. Neglecting the conductivity of negative ions compared to the electron conductivity and assuming that electrons mainly collide with molecular nitrogen, the electron density can be derived from an explicit relation [Banks and Kockarts, 1973]. The ion mobility depends upon the ion mass. Numerical models predict a mean ionic mass in the range 50–150 amu [Molina-Cuberos et al., 1999a], although more massive

ions are not excluded. We use a functional equation for the ion mobility [Meyerott et al., 1980] to calculate the relation between the positive ion concentration and the related conductivity.

[15] Figure 2 shows the densities of positive ions and electrons. The concentration of electrons is not equal to that of positive ions and the ratio ions/electrons decreases with altitude, from 300 (at ~ 135 km) to 5 (at ~ 70 km). There are no measurements of σ^+ below 70 km. The error bars associated with the concentration of positive ions, were calculated by considering the error in the numerical fitting and the uncertainties in the mass of ions, in the range 50–150 amu. The concentration of electrons at each altitude has been determined by the average between the determination obtained from the MI and RP techniques. The error bars include the range of variations between the two independent methods of measurement.

3. Discussion

[16] The negative branch of the conductivity measured by the RP2 is driven mostly by electrons, whose mobility is several orders of magnitude larger than that of negative ions, and can be compared with the conductivity measured by MI that is also driven by electrons [Hamelin et al., 2007]. However, the peak conductivity measured by MI is twice as large as that measured by RP. The reason for such a discrepancy is manifold.

[17] 1. The MI and RP measurements are not simultaneous. MI is operated during 2 s every 60 s, whereas a relaxation cycle of a given type lasts 56 s and is repeated every ~ 4 min. A sharp conductivity peak is therefore not seen with the same resolution by MI and RP.

[18] 2. The Probe descent velocity influences the MI results; this effect has been taken into account to some extent by Hamelin et al. [2007]. Due to the complexity of the MI probe configuration, the residual error in the determination of the electron density could be of the order of 20%.

[19] 3. Space charge effects are most important at 60 km, where the Debye length is of the order of only 3 cm, and

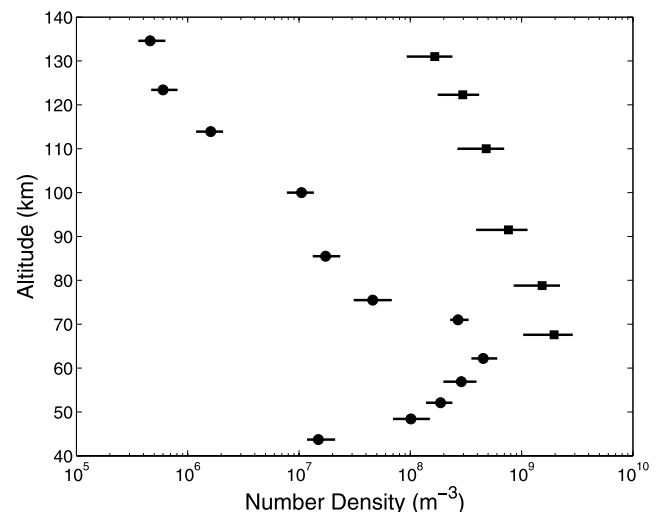


Figure 2. Density of positive ions (squares) and electrons (circles).

have been taken into account in the derivation of the RP results. The Probe descent velocity should not affect the relaxation response, because it is much less than the electron drift velocity associated with the relaxation electric field.

[20] 4. In spite of its relatively large surface area, the Huygens vehicle body is not a stable voltage reference, due to the large difference between the ion and electron conductivities. Interactions between the body and the RP1 and RP2 electrodes tend to negatively bias the potential of the former, which in turn repels the electron population in the vicinity of the relaxation sensors.

[21] In summary, the factor of 2 difference between the RP and MI electron conductivity measurements is compatible with the approximations made in the analyses of the two data sets. It is concluded that this fair agreement validates the determination of the conductivity peak altitude and amplitude, and the derivation of the electron density profile, down to an altitude of 40 km, by two totally different experimental approaches.

[22] The electron concentration is much lower than the one predicted by theoretical models and also lower than the ion concentration. The altitude of the electron density peak lies at around 60–70 km, not far from the theoretical prediction for maximum ionization rate by cosmic rays by *Molina-Cuberos et al.* [1999b] or K. O'Brien (personal communication, 2007) [Borucki and Whitten, 2008, Figure 6]; however, the peak density is $(460 \pm 110) \times 10^6 \text{ m}^{-3}$, about 4 times lower than that predicted by most models. Above 65 km, the electron density decreases with altitude much faster than predicted by theoretical models. The distribution of positive ions shows a concentration decreasing with altitude, with a maximum concentration of $(2 \pm 1) \times 10^9 \text{ m}^{-3}$ at around 65 km. Below this level the conductivity falls under the sensitivity threshold of the RP. Between 65 and 80 km the concentration of positive ions is in agreement with an ionosphere mainly formed by cluster ions [Molina-Cuberos et al., 1999a]. However, above 80 km the concentration of cations decreases with altitude much faster than expected with electron recombination. It is therefore necessary to include in the models other cation removal processes, such as aerosol capture.

[23] The lower value of the electron concentration compared with that predicted by theoretical models can be explained if an important fraction of the negative charges is attached to massive species (such as molecules and aerosols), which are less mobile than electrons and bring a negligible contribution to the conductivity. Ionospheric models take into account various processes that reduce the electron concentration. Negative ions can be produced by three body electron capture, with a rate that increases with density and is important at low altitude, below ≈ 70 km [Molina-Cuberos et al., 2000]. The presence of small embryos reduces the conductivity above 50 km [Borucki and Whitten, 2008] and thus the electron density. Monomers and polymers of poly-aromatic hydrocarbons are electrophilic species that could be very abundant above 120 km [Bakes, 2002]. Aerosols are abundant in the Titan atmosphere [Israël et al., 2005]. The effect on the electron concentration is to be reduced by electron capture and to be increased by daytime photoemission. The results obtained here show that the production of photoelectrons

should be very small, and aerosols reduce the concentration of electrons and positive ions.

4. Conclusions

[24] The relaxation technique has been used to determine the electrical conductivities due to positive and negative charges in the lower part of the atmosphere of Titan. The results obtained by the RP sensors are in agreement with the ones measured by the MI sensor using an independent method. Both sets of sensors indicated an ionised layer between 40 and 140 km. Here we present the number density profiles of positive ions and electrons. The distribution of positive ions, derived from the positive branch of the conductivity, shows a concentration decreasing with altitude, with a maximum of $\approx 2 \times 10^9 \text{ m}^{-3}$ at ≈ 65 km, below this altitude the conductivity falls under the sensitivity threshold. The electron density, derived from RP and MI measurements, is much lower than the positive ions density, which indicates that some negative charge is attached into more massive species, probably aerosols. Electron density peaks at ≈ 65 km, with a density of $\approx 450 \times 10^6 \text{ m}^{-3}$, and decreases with altitude much faster than positive ions. The electron and positive ions profiles are not in full agreement with existing models, the discrepancies could be explained in terms of aerosols physics, atmospheric chemistry and cloud dynamics.

[25] **Acknowledgments.** This work was supported by contracts ESP2003-00357 and ESP2006-02934. The authors thank all the national and international institutions that made the success of this experiment possible and especially International Space Science Institute for hosting their working-team meetings.

References

- Bakes, E. L. O. (2002), Photoelectric charging of submicron aerosols and macromolecules in the Titan haze, *Icarus*, 157, 464–475, doi:10.1006/icar.2002.6843.
- Banks, W. H., and G. Kockarts (1973), *Aeronomy*, Academic, New York.
- Bird, M. K., et al. (1997), Detection of Titan's ionosphere from Voyager 1 radio occultation observations, *Icarus*, 130, 426–436, doi:10.1006/icar.1997.5831.
- Borucki, W. J., and R. C. Whitten (2008), Influence of high abundances of aerosols on the electrical conductivity of the Titan atmosphere, *Planet. Space Sci.*, 56, 19–26.
- Borucki, W., et al. (1987), Predictions of the electrical conductivity and charging of the aerosols in Titan's atmosphere, *Icarus*, 72, 604–622.
- Coates, A. J., F. J. Crary, G. R. Lewis, D. T. Young, J. H. Waite Jr., and E. C. Sittler Jr. (2007), Discovery of heavy negative ions in Titan's ionosphere, *Geophys. Res. Lett.*, 34, L22103, doi:10.1029/2007GL030978.
- Cravens, T. E., et al. (2006), Composition of Titan's ionosphere, *Geophys. Res. Lett.*, 33, L07105, doi:10.1029/2005GL025575.
- Fischer, G., D. A. Gurnett, W. S. Kurth, W. M. Farrell, M. L. Kaiser, and P. Zarka (2007), Nondetection of Titan lightning radio emissions with Cassini/RPWS after 35 close Titan flybys, *Geophys. Res. Lett.*, 34, L22104, doi:10.1029/2007GL031668.
- Fulchignoni, M., et al. (2005), In situ measurements of the physical characteristics of Titan's environment, *Nature*, 438, 785–791, doi:10.1038/nature04314.
- Godard, R. (2007), Sheath and potential profiles around RP sensors and the gondola in the Huygens experiment, paper presented at the COMSOL Conference 2007, COMSOL, Boston, Mass.
- Grard, R., et al. (2006), Electric properties and related physical characteristics of the atmosphere and surface of Titan, *Planet. Space Sci.*, 54, 1124–1136, doi:10.1016/j.pss.2006.05.036.
- Gupta, S., et al. (1981), Organic synthesis in the atmosphere of Titan, *Nature*, 293, 725–727.
- Hamelin, M., et al. (2007), Electron conductivity and density profiles derived from the mutual impedance probe measurements performed during the descent of Huygens through the atmosphere of Titan, *Planet. Space Sci.*, 55, 1964–1977.

- Israël, G., et al. (2005), Complex organic matter in Titan's atmospheric aerosols from in situ pyrolysis and analysis, *Nature*, **438**, 796–799, doi:10.1038/nature04349.
- Kliore, A. J. (2007), The structure of the Titan ionosphere, *Bull. Am. Astron. Soc.*, **39**, 530.
- López-Moreno, J. J., et al. (2002), Polar ionic conductivity profile in fair weather conditions. Terrestrial test of the Huygens/Hasi-PWA instrument aboard the Comas Solá balloon, *J. Atmos. Sol. Terr. Phys.*, **63**, 1959–1966.
- López-Moreno, J. J., et al. (2002), The Comas sola mission to test the HUYGENS/HASI instrument on board a stratospheric balloon, *Adv. Space Res.*, **30**, 1359–1364.
- Mahaffy, P. R. (2005), Intensive Titan exploration begins, *Science*, **308**, 969–970, doi:10.1126/science.1113205.
- Meyerott, R. E., J. B. Reagan, and R. G. Joiner (1980), The mobility and concentration of ions and the ionic conductivity in the lower stratosphere, *J. Geophys. Res.*, **85**, 1273–1278.
- Molina-Cuberos, G. J., J. J. López-Moreno, R. Rodrigo, and L. M. Lara (1999a), Chemistry of the galactic cosmic ray induced ionosphere of Titan, *J. Geophys. Res.*, **104**, 21,997–22,024.
- Molina-Cuberos, G. J., et al. (1999b), Ionization by cosmic rays of the atmosphere of Titan, *Planet. Space Sci.*, **47**, 1347–1354.
- Molina-Cuberos, G. J., J. J. López-Moreno, and R. Rodrigo (2000), Influence of electrophilic species on the lower ionosphere of Titan, *Geophys. Res. Lett.*, **27**, 1351–1354.
- Ogawa, T. (1985), Fair-weather electricity, *J. Geophys. Res.*, **90**, 5951–5960.
- Vuitton, V., et al. (2006), The nitrogen chemistry of Titan's upper atmosphere revealed, *Astrophys. J.*, **647**, L175–L178, doi:10.1086/507467.
- Wahlund, J.-E., et al. (2005), Cassini measurements of cold plasma in the ionosphere of Titan, *Science*, **308**, 986–989, doi:10.1126/science.1109807.
-
- C. Béghin, LPCE, CNRS, 3A, Avenue de la Recherche Scientifique, F-45071 Orléans CEDEX 2, France.
- J. J. Berthelier, M. Hamelin, and F. Simões, CETP, IPSL, 4, Avenue de Neptune, F-94107 Saint Maur CEDEX, France.
- V. J. G. Brown, J. M. Jerónimo, J. J. López-Moreno, and R. Rodrigo, Instituto de Astrofísica de Andalucía, CSIC, P.O. Box 3004, E-18080 Granada, Spain. (lopez@iaa.es)
- F. Ferri, CISAS “G. Colombo”, Università di Padova, Via Venezia 15, I-35131 Padova, Italy.
- M. Fulchignoni, LESIA, Observatoire de Paris, 5 Place Janssen, F-92195 Meudon CEDEX, France.
- R. Godard, Department of Mathematics and Computer Science, Royal Military College of Canada, Kingston, ON K7M 1Y6, Canada.
- R. Grard, P. Falkner, and R. Trautner, RSSD, ESTEC, European Space Agency, Keplerlaan 1, NL-2200 AG Noordwijk, Netherlands.
- I. Jernej and K. Schwingenschuh, Space Research Institute, OEAW, Schmiedlstrasse 6, A-8042 Graz, Austria.
- G. J. Molina-Cuberos, Electromagnetismo, Facultad de Químicas, Universidad de Murcia, Campus Espinardo, E-30100 Murcia, Spain.